

# Quantitative correlation of Lower Silurian carbonate facies in Lithuania: insights from carbon isotopes and cross-recurrence plots

TOMAS ŽELVYS, ANNA CICHON-PUPIENIS, ROBERTAS STANKEVIČ,  
ANDRIUS GARBARAS & SIGITAS RADZEVIČIUS

The practice of formalizing chemostratigraphic units and defining isotopic zones based on excursions has become widespread. For more than three decades, stable carbon isotopes have played an important role in the solution of Silurian stratigraphy.  $\delta^{13}\text{C}_{\text{carb}}$  data supplement other stratigraphical proxies, allowing the subdivision of geological sections and more precise correlation. In this paper we provide new  $\delta^{13}\text{C}_{\text{carb}}$  data from the Silurian section of the Ledai-179 borehole, which is located in central Lithuania. The lower Silurian geological succession of Ledai-179 well is composed of carbonate and sulfate deposits. Two positive carbon isotope excursions were identified in the Ledai-179 borehole: Ireviken and Mulde. In this study, we employed stable carbon isotope data from Ledai-179 and Jočionys-299 (Eastern Lithuania) boreholes and the cross recurrence plot as additional tools to compare two time series (Telychian–Homeric interval) in a data-point-wise manner. The results indicate that stable carbon isotope data exhibit sufficient temporal and spatial coherence to serve as a reliable additional tool for correlating geological sequences. • Key words: Llandovery, Wenlock,  $\delta^{13}\text{C}_{\text{carb}}$ , recurrence plots.

ŽELVYS, T., CICHON-PUPIENIS, A., STANKEVIČ, R., GARBARAS, A. & RADZEVIČIUS, S. 2025. Quantitative correlation of Lower Silurian carbonate facies in Lithuania: insights from carbon isotopes and cross-recurrence plots. *Bulletin of Geosciences* 100(4), 607–615 (4 figures, 1 electronic appendix). Czech Geological Survey, Prague. ISSN 1214-1119. Manuscript received July 4, 2025; accepted in revised form December 10, 2025; published online December 31, 2025; issued December 31, 2025.

Tomas Želvys (corresponding author), Robertas Stankevič & Sigitas Radzevičius, Department of Geology and Mineralogy, Vilnius University, M. K. Čiurlionio 21/27, LT-03101 Vilnius, Lithuania; tzelvys@gmail.com • Anna Cichon-Pupienis, Laboratory of Bedrock Geology, Nature Research Centre, Akademijos str. 2, 08412 Vilnius, Lithuania • Andrius Garbaras, Department of Nuclear Research, Center for Physical Sciences and Technology, 10221 Vilnius, Lithuania

Marine deposits carbon isotope stratigraphy provides a powerful tool for reconstructing past variations in the global carbon cycle and correlating sedimentary successions through time. The carbon on Earth is broadly divided between two main reservoirs: organic carbon, which is isotopically lighter due to its enrichment in  $^{12}\text{C}$ , and carbonate carbon, which is isotopically heavier, containing relatively more  $^{13}\text{C}$ . Variations in the burial and oxidation of organic matter regulate the isotopic balance between these reservoirs. The potential of marine carbonate  $\delta^{13}\text{C}$  values to date and correlate rocks relies on the fact that their  $^{13}\text{C}/^{12}\text{C}$  values have varied over time, mainly as the result of partitioning of carbon between organic carbon and carbonate carbon reservoirs in the lithosphere (e.g., Shackleton & Hall 1984, Berner 1990, Kump & Arthur 1999, Falkowski 2003, Sundquist & Visser 2004).

When large amounts of organic carbon are buried, the residual dissolved inorganic carbon (DIC) pool in the ocean becomes enriched in  $^{13}\text{C}$ , producing positive  $\delta^{13}\text{C}$

excursions in marine carbonates. Conversely, when organic carbon is oxidized and returns to the system,  $\delta^{13}\text{C}$  values decrease. Stable carbon isotopes as a chemostratigraphic tool are mostly used alongside lithostratigraphic, biostratigraphic data in stratigraphy

The first studies of stable carbon isotope variability in Silurian rocks started in the last decade of the last century (Corfield *et al.* 1992, Samtleben *et al.* 1996, Wenzel & Joachimski 1996, Kaljo *et al.* 1997). Stable carbon isotopes as a chemostratigraphic tool are mostly used alongside lithostratigraphic and biostratigraphic data in stratigraphy. During the last three decades, these studies have become very active and data of Silurian stable carbon isotopes is rapidly increasing around the world. It made possible to carry out generalized studies on the variability of carbon isotopes in the Silurian rocks (e.g., Cramer *et al.* 2011, Melchin *et al.* 2020).

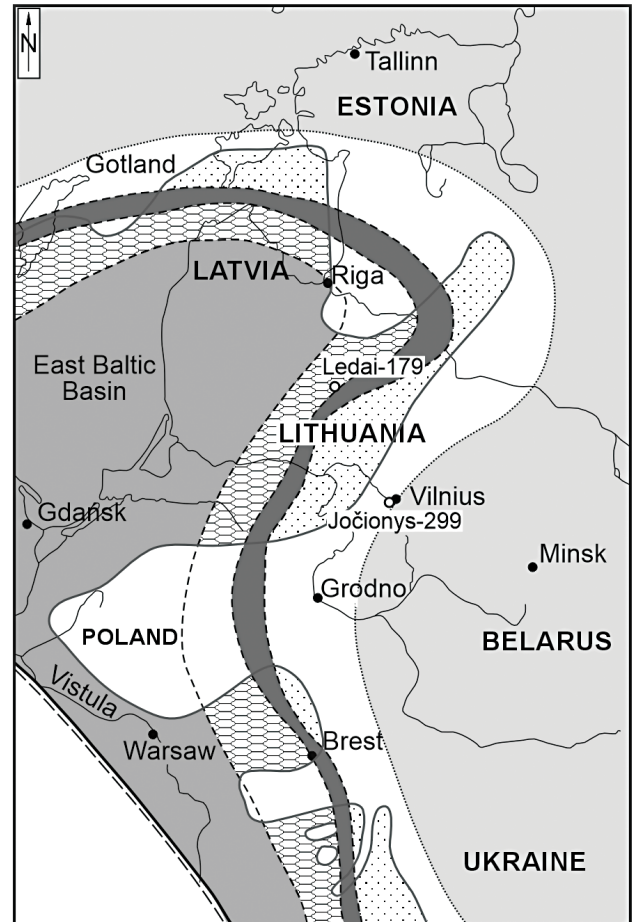
There are several stable carbon isotope ( $\delta^{13}\text{C}_{\text{carb}}$ ) variabilities determined based on the data of  $\delta^{13}\text{C}_{\text{carb}}$  from

whole rocks, carbonates, and organic material in the Llandovery and Wenlock (Telychian–Homerian interval), the lower Silurian. Some  $\delta^{13}\text{C}_{\text{carb}}$  excursions are very well documented elsewhere, others are still under discussion. The Kallholn (Walasek *et al.* 2018, Cichon-Pupienis *et al.* 2021), Valgu (Munnecke & Männik 2009), Sommerodde (Hammarlund *et al.* 2019, Loydell *et al.* 2023) and Manitowoc (McLaughlin *et al.* 2019, Yan *et al.* 2025)  $\delta^{13}\text{C}_{\text{carb}}$  excursions are distinguished in the Telychian. However, the stratigraphic position of Telychian carbon isotopes excursions is unclear, due to a lack of precise graptolites and conodont biostratigraphical data and more detailed future research is needed. The Wenlock positive  $\delta^{13}\text{C}_{\text{carb}}$  excursions are well known around the world and clearer. The early Sheinwoodian or the Ireviken positive  $\delta^{13}\text{C}_{\text{carb}}$  excursion is one of the biggest carbon isotope shifts during the Silurian (*e.g.*, Cramer *et al.* 2010, Radzevičius *et al.* 2024). The middle to latter Homerian or Mulde positive carbon isotope excursion is linked to the *P. parvus*–*Col. ludensis* biozones and is widely documented worldwide (*e.g.*, Rinkevičiūtė *et al.* 2021, Frýda & Frýdová 2025).

The purpose of this study is to document carbon isotopes trends in Central Lithuania, spanning the lower Silurian (Llandovery, Wenlock) and to integrate new carbon isotope data lithostratigraphy and biostratigraphy to correlate the carbonate facies from East Lithuania to those in Central Lithuania. The recurrence plots method as a supporting tool (*e.g.*, Eckmann *et al.* 1987, Spiridonov 2017) was used for correlation of problematic geological sections of shallow deposits in Lithuania. Recurrence plots are filtered distance matrices which visualize patterns of dynamics of the dynamic system and show time periods when system becomes similar to its previous states. In this paper we used cross-recurrence plot which is the product of comparison of two data series (Marwan & Kurths 2004). A cross-recurrence plot consists of recurrence points which shows the similarity across both data series, i.e. stratigraphical depths, and this helps further to correlate the series. Then we used a dynamic time warping algorithm which finds the minimal cost path across the plot, from corner to corner. This minimal cost path is interpreted as synchronization (geologic correlation) line. This method is successfully applied for correlation purposes (*e.g.*, Spiridonov *et al.* 2019, 2020; Stankevič *et al.* 2024).

## Geological setting

Lithuania was a part of the Baltica paleocontinent and was located near the equator in the southern hemisphere during the early Silurian (Cocks & Torsvik 2005). The Ledai-179 borehole was drilled in Central Lithuania



Legend:  
 Land areas (white)  
 Area of post-Silurian erosion (dotted)  
 Lagoon (stippled)  
 Barrier (solid black)  
 Inner shelf (horizontal lines)  
 Outer shelf (vertical lines)  
 Tornquist-Teisseyre Zone (dashed line)  
 Present erosional boundaries of Silurian deposits (solid line)  
 Reconstructed boundary of East Baltic Silurian Basin (dotted line)

**Figure 1.** The East Baltic Silurian Basin paleogeographic map during *Gothograptus nassa* (the middle Homerian, Wenlock) time (after Einasto *et al.* 1986) and location of the Ledai-176 and Jočionys-299 boreholes.

(Fig. 1) and crosses the shallow marine deposits of a Lower Silurian carbonate facies succession.

There are four distinguished formations, the Švenčionys, Paprieniai, Birštonas and Nevėžis (Fig. 2), based on based on lithological composition and gamma-ray log data in the investigated interval of the Ledai-179 borehole (Lapinskas 2000). The neostatotype of the Švenčionys Formation is in Ledai-179 well and it is composed by marlstone and represent Telychian Age (Brazauskas 1991). The Paprieniai Formation is early Sheinwoodian age and it is subdivided into the Sutkai and Vilkiija beds. The stratotypes of Sutkai and Vilkiija beds are in the Ledai-179 borehole (Sidaravičienė *et al.* 1999). The Sutkai beds are composed by greenish and dark grey marlstone. The Vilkiija beds are composed by

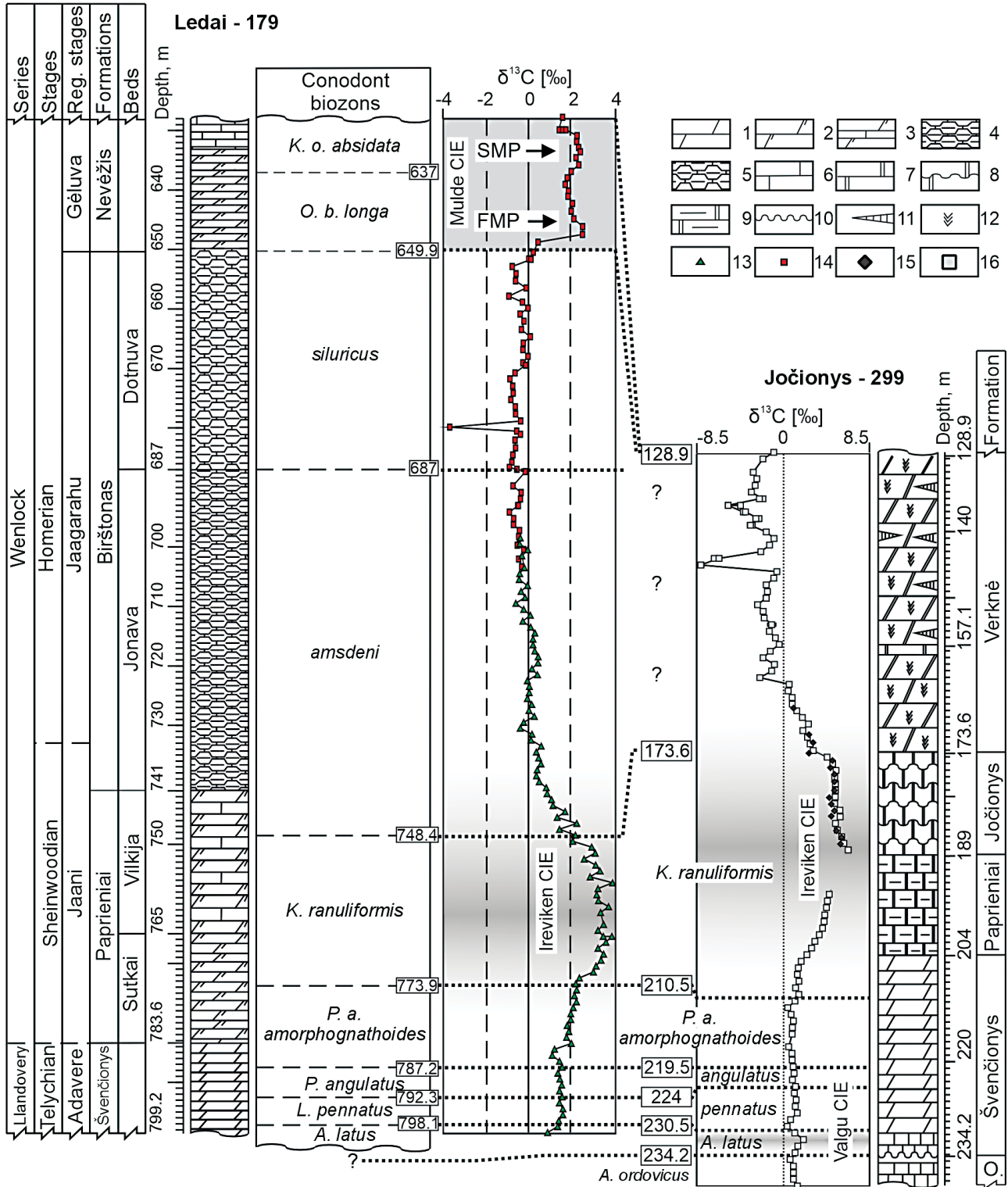


**Figure 2.** Lithology, conodont biozones and stable carbon isotopic curve of the Ledai-179 borehole (this paper) and correlation with him of the Jočionys-299 borehole (Želvys et al. 2022). Abbreviations: CIE – carbon isotope excursion; O. – Ordovician; Reg. Stage – Regional Stage (after Paškevičius et al. 1994). Legend: 1 – marlstone; 2 – dolomitic marlstone; 3 – marlstone with limestones interbeds; 4 – nodular limestone with marlstone interbeds; 5 – nodular limestone; 6 – limestone; 7 – dolostone; 8 – wavy laminated dolostone; 9 – argillaceous dolostone; 10 – hardground; 11 – gypsum interbeds; 12 – reddish in color. Carbon isotopes: 13 – this paper; 14 – Radzevičius et al. (2014); 15 – Kaminskas et al. (2010); 16 – Želvys et al. (2022).

grey marlstone with limestones interbeds. The Birštonas Formation is latter Seinwoodian and early Homeric age (Brazauskas 1991) and the neostatotype of the formation is in the Ledai-179 well. There are distinguished Jonava and Dotnuva beds in the Birštonas Formation. The Jonava beds are composed by nodular limestone with marlstone interbeds and the Dotnuva beds are composed by nodular limestone (Fig. 2). In the Ledai-179 well, the stratotype of the Nevėžis Formation is also present. The Nevėžis Formation is composed by clayey dolostone with gypsum and dolomitic limestone on top. The Nevėžys Formation was thought to be of Gorstian Age previously (e.g., Paškevičius *et al.* 1994), but new data places the Nevėžis Formation in the Homeric (Radzevičius *et al.* 2017, Spiridonov *et al.* 2017a, b).

Several lower Silurian conodont biostratigraphic studies have been conducted on the Ledai-179 well (Paškevičius & Brazauskas 1987, Brazauskas 1991, Spiridonov *et al.* 2015). The *Aulacognathus latus*, *Pterospathodus pennatus*, *Pterospathodus amorphognathoides angulatus* and *Pterospathodus amorphognathoides amorphognathoides* conodont biozones of Telychian are distinguished in the Ledai-179 borehole. *Kockelella ranuliformis*, *Kockelella amsdeni*, *Oulodus siluricus*, *Ozarkodina bohémica longa* and *Kockelella ortus absidata* conodont biozones were distinguished in the upper part of the investigated interval of the Ledai-179 well and marks the Wenlock.

There are a few findings of thelodonts and acanthodians documented in the lower Silurian of Ledai-179 borehole (Karatajūtė-Talimaa *et al.* 1987). The Thelodonts *Logania* sp. and *Thelodus* sp. nov. have been found in the Nevėžis Formation.

Kaminskas (2001) conducted a geochemical (trace and major elements) and mineralogical investigation of the Wenlock interval of Ledai-179.  $\delta^{13}\text{C}_{\text{carb}}$  and  $\delta^{18}\text{O}$  composition of the upper Wenlock were investigated by Radzevičius *et al.* (2014) which identified the Mulde stable carbon isotope excursion.

## Material and methods

**Isotope analyses.** – New material for stable carbon isotope analyses were taken from the 798.5–679.9 m depth interval from the Ledai-179 borehole core. Samples were collected at approximately 1 m resolution. Collected rocks were ground into powder prior to measurement.

The stable carbon isotope composition was analyzed using traditional techniques (e.g., Rinkevičiūtė *et al.* 2021) by the Thermo Gasbench II in tandem with the Thermo Delta V isotope ratio mass spectrometer at the Nuclear Research Department of the State Research Institute Center of Physical Sciences and Technology, Vilnius. All samples were loaded into 10 mL Labco Exetainer vials,

flushed with He, and later treated with 99.99%  $\text{H}_3\text{PO}_4$  at 50 °C for 10 h. The isotope data were normalized against the reference materials IAEA-CO-8 ( $\delta^{13}\text{C}_{\text{carb}} = -5.764 \pm 0.032\%$ ) and NBS 18 ( $\delta^{13}\text{C}_{\text{carb}} = -5.014 \pm 0.035\%$ ). The standard deviation ( $1\sigma$ ) for the sample analyses was 0.06%.

**Cross-recurrence plot and synchronization.** – In order to correlate the studied geological sections, we compared  $\delta^{13}\text{C}_{\text{carb}}$  time series and constructed a cross-recurrence plot. Then we used a dynamical time warping (DTW) algorithm which finds a minimal cost path on a cross-recurrence plot, which we interpret as a line of synchronization (i.e., correlation). The DTW algorithm has been successfully applied to the geological correlation of geophysical logs in geologically similar environments, sometimes across significant distances (Hladil *et al.* 2010, 2011), and even to studying Ludlow successions in the Prague Basin (Chadimová *et al.* 2015). DTW on cross-recurrence plots used to correlate Wenlock–Ludlow successions by compositions of paleoecological communities (Spiridonov *et al.* 2020).

**Recurrence and cross-recurrence plots.** – An auto-recurrence plot, or simply – recurrence plot (RP), would be obtained by comparison of a single time series with itself (Eckmann *et al.* 1987, Marwan *et al.* 2007). Square matrix of all possible pair-wise comparison is obtained by applying chosen distance metric. Two perpendicular axes of the matrix account for time dimension: time flows from left to right and bottom-up, therefore, the diagonal is the identity line and the symmetry axis (only for auto-RP). In this particular case, the time line spanning from Telychian to Homeric is covered. Filtering a distance matrix with binary step function converts it to a recurrence plot: similar states are coded “1” (the black pixels on the plot) and differing states are coded “0” (the white pixels on the plot). Mathematically, a recurrence plot can be expressed in the following way (Webber & Marwan 2015, Spiridonov *et al.* 2017b):  $R_{ij}(\epsilon) = \theta(\epsilon - d_{ij})$ , for  $i, j = 1, \dots, N$ ; here,  $R_{ij}$  – point on a recurrence plot;  $\theta(\cdot)$  – Heaviside step function;  $\epsilon$  – threshold level of similarity;  $d_{ij}$  – normed distance or difference between the states at times;  $i$  and  $j$  – i.e., values  $x_i$  and  $x_j$  of the time series  $x$ .

In the same way, by comparing two neighboring (or related) stratigraphical series, we obtain a cross-recurrence plot (CRP). As a rule, the matrix or the plot is not equisided (Marwan *et al.* 2002; Marwan & Kurths 2002, 2004):  $\text{CR}_{ij}(\epsilon) = \theta(\epsilon - d(x_i, y_j))$ , for  $i = 1, \dots, N, j = 1, \dots, M$ ; here,  $\text{CR}_{ij}(\epsilon)$  is a point on a rectangular ( $N \times M$ ) cross-recurrence plot comparing two time points  $x_i$  and  $y_j$  of time series  $x$  and  $y$  respectively, which are sample series of  $\delta^{13}\text{C}_{\text{carb}}$  values from two studied cores. The distance metric we used is an absolute value of a difference between

$\delta^{13}\text{C}_{\text{carb}}$  values after one time series (Jočionys-299) were normalized to another one (Ledai-179). Normalization was done by changing absolute variability to be the same in both series, and translating values so that the averages match. Specifically, a new value was obtained by subtracting the series average from an old value, multiplying it by the ratio between absolute variabilities, and finally adding the average of another series.

The threshold value ( $\epsilon$ ) was automatically adjusted so that the studied cross-recurrence plot would have a 30% recurrence rate. Using smaller recurrence rates produced similar plots with similar coarse geometric patterns, and we pick 30% as these patterns appeared saturated. Increasing recurrence rate further the  $\epsilon$  values becomes too low and some new places with geometric patterns start to appear bearing lower recurrence values.

The structures consisting of recurring points that appear on the recurrence (and cross-recurrence) plot can indicate the system's dynamical features. Horizontal and vertical lines represent unchanging and very similar (so-called "laminar") states (Marwan *et al.* 2007). Diagonal lines represent deterministic states of a system, which means that a system visits the same portions of state spaces, and is thus attracted to this portion of the total state space.

*Obtaining synchronization line.* – In order to obtain the line of synchronization on the cross-recurrence plot, an algorithm should evaluate structures of recurrence around the main diagonal. Best case scenario is a comparison of two identical time series, which reduces to an auto-recurrence plot, thus the line of synchronization strictly coincide with the main diagonal, so-called line of identity  $R_{ij} = 1$ , for all  $i$ . Paleontological or geochemical data series are geologically distorted because of the unevenness of the sedimentation and erosion, thus the real timeline of isochronous events represented as a line of synchronization can be very uneven, deviating from the main diagonal of cross-recurrence plot by significant distances, and local tangents of the line can often vary greatly from 0 to 90 degrees during the episodes of erosion and hiatuses in the paleo-terrain of one of the two series (Spiridonov *et al.* 2017b).

We used the Dynamical time warping (DTW) algorithm. It is an iterative numerical algorithm, which finds the path on the matrix with the minimal overall cost (synchronization line). The algorithm dynamically fills the new matrix of minimal costs using the matrix of distances (Heaviside-filtered matrix or recurrence plot in our case). We used the standard algorithm, where every next empty cell of the minimal costs matrix is filled with the cost of the distance matrix (CRP) cell plus the minimum of the three previously calculated neighboring cells values, *i.e.*,  $\text{DTW}_{ij} = \text{cost} + \min(\text{DTW}_{i-1,j}, \text{DTW}_{i,j-1}, \text{DTW}_{i-1,j-1})$ . Then the minimal cost path on the matrix (plot) consists

of adjacent points (including diagonally adjacent) and the line is non-decreasing regarding both axes. The algorithm works from predetermined starting and ending points at the corners of the matrix (plot), therefore we assume that we have two pairs of points (starting and ending) of the analyzed data series that are already approximately correlated. The algorithm finds one synchronization line, although several paths can be similar by their overall costs. Normally, the wide areas with high local recurrence rate (laminar states) add some uncertainty about the power of the single best synchronization line. And usually, the narrow diagonal junctions between wide areas of recurrence (interpreted as mutual abrupt state shifts) increase the confidence of correlation line. Changing the global recurrence rate of the cross-recurrence plot of the studied series generates a variety of synchronization lines. These lines are quite similar across CRPs but wander in the areas within laminar states (highly filled rectangle-shaped areas in CRP), therefore the confidence is lower at these subintervals. In laminar states the algorithm produces similar cost paths in the costs matrix, *e.g.*, on completely filled 45 degree parallelogram all shortest paths between far angles are of the same length and of the same cost.

## Carbon isotopes

The lowermost Silurian  $\delta^{13}\text{C}_{\text{carb}}$  excursion starts from 0.8‰ at 798.5 m depth. The values remain very similar throughout the Švenčionys Formation up to 784.5 m where the value is 1.2‰ (Fig. 2). From 784.5 m, the values increase rapidly to 3.38‰ at 765.5 m depth. In the 765.5–751.5 m interval (Paprieniai Formation),  $\delta^{13}\text{C}_{\text{carb}}$  values vary slightly around 2.5–3.8‰.  $\delta^{13}\text{C}_{\text{carb}}$  values gradually fall from the upper part of the Paprieniai Formation from 3.03 ‰ at 751.5 m depth to 0.11‰ at 731.5 m depth of the lower part of Jonava beds and then are moderately stable for the 730–670 m depth interval (vary from 0.12 ‰ to –0.64‰).

Thereafter,  $\delta^{13}\text{C}_{\text{carb}}$  values rapidly increase to 2.47‰ at 646.1 m depth (Nevėžis Formation), and fall to 1.66‰ at 639 m. Again,  $\delta^{13}\text{C}_{\text{carb}}$  rise to 2.29‰ 635.7 m depth and fall to 1.54‰ in the uppermost part of the Nevėžys Formation in Ledai-179 borehole.

## Discussion

The succession of conodont biozones from *A. latus* to *K. o. absidata* established in the Ledai-179 well (Fig. 2) indicates that the geological section spans from the early Telychian (Llandovery) to the late Homerian (Wenlock). So, geological section is quite complete without big stratigraphical gaps in Ledai-179 borehole (Central Lithuania).

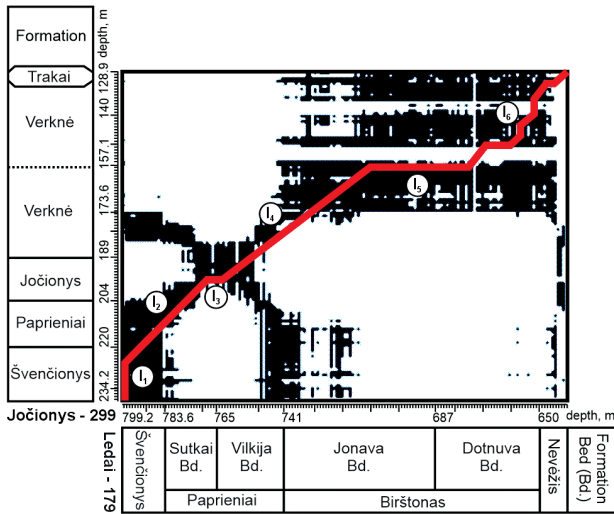


**Figure 3.** Cross-recurrence plots of  $\delta^{13}\text{C}_{\text{carb}}$  data with estimated synchronization (stratigraphical correlation) line (red line) of Jočionys-299 and Ledai-179 boreholes. Legend:  $I_n$  – intervals of the graphic correlation line.

The Lower Silurian geological section of the Jočionys-299 well is not so complete. There are distinguished conodont biozones from *A. latus* to *K. ranuliformis* and this continuous sequence of conodont biozones shows the ages of the Telychian and the Sheinwoodian (Fig. 2). In the Verknė Formation of the Jočionys-299 borehole the

conodont and other important fauna are absent. This makes the correlation of the Verknė Formation complicated.

Based on stable carbon isotope ( $\delta^{13}\text{C}_{\text{carb}}$ ) data, the Ireviken and Mulde positive carbon isotope excursions (CIE) are identified in the Ledai-179 well (Fig. 2). The Ireviken ICE began at the Llandovery Wenlock boundary and is relate to the Sheinwoodian. In the Ledai-179 borehole, the Mulde CIE with its characteristic two positive  $\delta^{13}\text{C}_{\text{carb}}$  peaks was identified in the upper Homerian (Radzevičius *et al.* 2014). Two positive carbon isotope excursions were determined in the Jočionys-299 borehole (Želvys *et al.* 2022). The Valgu CIE is established in the lower part of Švenčionys Formation (lower Telychian) and it is related with a thin layer of limestone of the Formation (Fig. 2). The Ireviken CIE is also distinguished there. Thus, the uppermost Homerian deposit is absent and there is a large stratigraphic gap between the Verknė (Homerian) and the Trakai (Gorstian) formations (Fig. 4).

Biostratigraphic data and chemostratigraphic data are complementary to each other and are felt to compose an overall view. However, the Verknė Formation correlation is still unclear. To uncover some insights, the cross-recurrence plot and dynamical synchronization methods were used as additional tools (Fig. 3). Stable carbon  $\delta^{13}\text{C}_{\text{carb}}$  isotope data from both cores were compared and the cross-recurrence plot was generated. The line of synchronization

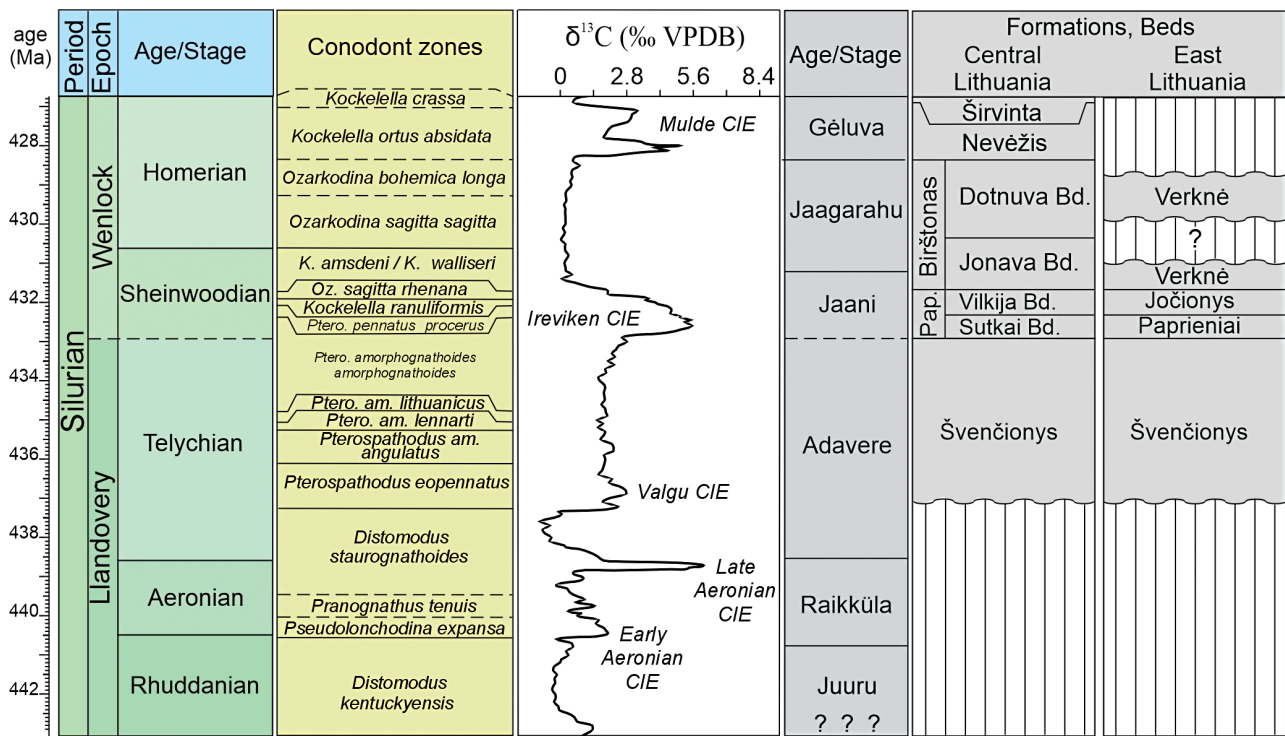


**Figure 4.** Silurian time scale, conodont zonation, generalized  $\delta^{13}\text{C}_{\text{carb}}$  curve (Melchin *et al.* 2020) and Lithuanian regional stages correlation with lithostratigraphic units of the Ledai-179 (central Lithuania) and Jočionys-299 (eastern Lithuania) boreholes.

(i.e., correlation) was obtained by Dynamic time warping (DTW) algorithm. Besides diagonal segments, there are several horizontal and vertical intervals. We interpret these intervals as unconformities, but it is important to note, that all of them are of lesser confidence, because they appear in rectangular recurrence states.

The whole Line of Graphic Correlation (Fig. 3) can be divided into at least 6 episodes ( $I_{1,2,3,4,5,6}$ ; Fig. 3). Nonetheless, we can discuss the non-diagonal intervals, which are the most important for our purposes, albeit with caution. The first interval ( $I_1$ ) of correlation line indicates the possible unchanging or unconformity in the lower part of the Ledai-179  $\delta^{13}\text{C}_{\text{carb}}$  data (Fig. 3). There is determinate the Valgu CIE in Jočionys-299 well, but this CIE is absent in investigated interval of Ledai-179 well. This is due to the fact that samples from the uppermost Ordovician and the lowermost part of the Švenčionys Formation were not taken from Ledai-179 well core. The geological section of the Švenčionys Formation is more complete in the Jačionys-299 well in this case. The second horizontal interval ( $I_2$ ) of correlation line may be related to the Ireviken CIE and is related to the sampling gap in Jočionys-299 borehole (Fig. 3). According to the Lithuanian core storage information, the 194–188 m interval of the Jočionys-299 well core was missed (Želvys et al. 2022). The third horizontal interval ( $I_3$ ) of correlation line is related (although with low confidence) to the middle part of the Verknė Formation (Fig. 4). So, the stratigraphical gap could be between the lower and the upper members of Verknė Formation. This stratigraphic hiatus is associated with a fall in sea level in the Baltic palaeobasin (Männik et al. 2024) and linking to later Jaagarahu Age. A modest sea-level fall following the Ireviken Event has been documented globally (Loydell 1998).

The upper parts of both cores are not known to end at the same time, therefore we cannot meaningfully analyze the very top (top-right corner) of the recurrence plot.

## Conclusions

The Ireviken positive carbon excursion is well recorded in Ledai-179 borehole. The highest value of is  $\delta^{13}\text{C}_{\text{carb}}$  3.84‰ (Paprieniai Formation) and is lower than in shallow facies of Jočionys-299 well ( $\delta^{13}\text{C}_{\text{carb}}$  6.4‰).

A stratigraphic gap in the middle part of the Verknė Formation in eastern Lithuania can be identified by correlating the isotope data from the Ledai-179 and Jočionys-299 wells using cross-recurrence analysis.

The cross-recurrence analysis, used as an additional mathematical method and combined with traditional lithostratigraphical, biostratigraphical, and chemostratigraphical methods, is an effective tool for refining stratigraphy and correlating borehole successions.

## Acknowledgments

This is a contribution to the project entitled ‘Rocks and the Rise of Ordovician Life’ (IGCP 735). Authors were supported by the Lithuania Research Council grants: S-MIP-24-62 “BretEvoGeneralized” (Robertas Stankevič) and P-MIP-23-129 “Shifts in the paleoenvironments during the early Paleozoic – tracking the turning points in climate and insight into the depositional environments” (Anna Cichon-Pupienis). Jiří Frýda and an anonymous reviewer made this a stronger manuscript.

## References

- BERNER, R.A. 1990. Atmospheric carbon dioxide levels over Phanerozoic time. *Science* 249, 1382–1386. DOI 10.1126/science.249.4975.1382
- BRAZAUSKAS, A. 1991. Lietuvos silūro konodontų asociacijos. *Geologija* 12, 67–76.
- CHADIMOVÁ, L., VACEK, F., SOBIEN, K., SLAVÍK, L. & HLADIL, J. 2015. Petrophysical record of the Late Silurian shallow-water carbonate facies across the Lau Event (Prague Synform, Czech Republic) and dynamic time warping alignment of the magnetic susceptibility logs. *Geological Society London, Special Publication 414(1)*, 133–155. DOI 10.1144/SP414.14
- CICHON-PUPIENIS, A., LITKE, R., LAZAUSKIENĖ, J., BANIASAD, A., PUPIENIS, D., RADZEVIČIUS, S. & ŠLIAUSKAS, L. 2021. Geochemical and sedimentary facies study – Implication for driving mechanisms of organic matter enrichment in the lower Silurian fine-grained mudstones in the Baltic Basin (W Lithuania). *International Journal of Coal Geology* 244, 103815. DOI 10.1016/j.coal.2021.103815
- COCKS, L.R.M. & TORSVIK, T.H. 2005. Baltica from the late Precambrian to mid-Palaeozoic times: the gain and loss of a terrane’s identity. *Earth-Science Reviews* 72, 39–66. DOI 10.1016/j.earscirev.2005.04.001
- CORFIELD, R.M., SIVETER, D.J., CARLIDGE, J.E. & MCKERROW, W.S. 1992. Carbon isotope excursion near the Wenlock–Ludlow (Silurian) boundary in the Anglo–Welsh area. *Geology* 20(4), 371–374. DOI 10.1130/0091-7613(1992)020<0371:CIENTW>2.3.CO;2
- CRAMER, B.D., LOYDELL, D.K., SAMTLEBEN, C., MUNNECKE, A., KALJO, D., MANNIK, P., MARTMA, T., JEPSSON, L., KLEFFNER, M.A., BARRICK, J.E., JOHNSON, C.A., EMSBO, P., JOACHIMSKI, M.M., BICKERT, T. & SALTZMAN, M.R. 2010. Testing the limits of Paleozoic chronostratigraphic correlation via high-resolution (<500 kyr) integrated conodont, graptolite and carbon isotope ( $\delta^{13}\text{C}_{\text{carb}}$ ) biochemostratigraphy across the Llandovery–Wenlock (Silurian) boundary: Is a unified Phanerozoic timescale achievable? *Geological Society of America Bulletin* 122(9–10), 1700–1716. DOI 10.1130/B26602.1
- CRAMER, B.D., BRETT, C.E., MELCHIN, M.J., MÄNNIK, P., KLEFFNER, M.A., MCLAUGHLIN, P.I.; LOYDELL, D.K., MUNNECKE, A., JEPSSON, L., CORRADINI, C., BRUNTON, F.R. & SALTZMAN, M.R. 2011. Revised correlation of Silurian

- Provincial Series of North America with global and regional chronostratigraphic units and  $\delta^{13}\text{C}_{\text{carb}}$  chemostratigraphy. *Lethaia* 44(2), 185–202. DOI 10.1111/j.1502-3931.2010.00234.x
- ECKMANN, J.P. KAMPHORST, S.O. & RUELLE, D. 1987. Recurrence plots of dynamical systems. *Europhysics Letters* 4, 973–977. DOI 10.1209/0295-5075/4/9/004
- EINASTO, P.E., ABUSHIK, A.F., KALJO, D.L., KOREN, T.N., MODZALEVSKAYA, T.L. & NESTOR, H.E. 1986. Osobiennosti silurskoho osadkonakopenija i asociacii fauny w kraevykh bassejnach Pribaltiki i Podolii. *Teoria i opyt ekostratigrafii*, 65–72. [in Russian]
- FALKOWSKI, P. 2003. Biogeochemistry of Primary production in the Sea. *Treatise on Geochemistry* 8, 185–213. DOI 10.1016/B0-08-043751-6/08129-9
- FRÝDA, J. & FRÝDOVÁ, B. 2025. High-resolution records of the mid-Homerian (Silurian) marine chemistry evolution and graptolite biodiversity across the Lundgreni Event reveal what nearly killed the graptolites. *Palaeogeography, Palaeoclimatology, Palaeoecology* 668, 112866. DOI 10.1016/j.palaeo.2025.112866
- HAMMARLUND, E.U., LOYDELL, D.K., NIELSEN, A.T. & SCHOVSBO, N.H. 2019. Early Silurian  $\delta^{13}\text{C}_{\text{org}}$  excursions in the foreland basin of Baltica, both familiar and surprising. *Palaeogeography, Palaeoclimatology, Palaeoecology* 526, 126–135. DOI 10.1016/j.palaeo.2019.03.035
- HLADIL, J., VONDRA, M., ČEJCHAN, P., ROBERT, V., KOPTÍKOVÁ, L. & SLAVÍK, L. 2010. The dynamic time-warping approach to comparison of magnetic-susceptibility logs and application to lower Devonian calciturbidites (Prague Synform, Bohemian Massif). *Geologica Belgica* 13(4), 385–406.
- HLADIL, J., SLAVÍK, L., VONDRA, M., KOPTÍKOVÁ, L., ČEJCHAN, P., SCHNABL, P., ADAMOVIČ, J., VACEK, F., VÍCH, R. & LISÁ, L. 2011. Pragian–Emsian successions in Uzbekistan and Bohemia: magnetic susceptibility logs and their dynamic time warping alignment. *Stratigraphy* 8(4), 217–235. DOI 10.29041/strat.08.4.01
- KALJO, D., KIIPLI, T. & MARTMA, T. 1997. Carbon isotope event markers through the Wenlock–Pridoli sequence at Ohesaare (Estonia) and Priekule (Latvia). *Palaeogeography, Palaeoclimatology, Palaeoecology* 132, 211–223. DOI 10.1016/S0031-0182(97)00065-5
- KAMINSKAS, D. 2001. Geochemical peculiarities of the Wenlock (Lower Silurian) rocks in Ledai-179 and Jocionys-299 boreholes (E. Lithuania). *Geologija* 35, 3–14.
- KAMINSKAS, D., BIČKAUSKAS, G. & BRAZAUSKAS, A. 2010. Silurian dolostones of eastern Lithuania. *Estonian Journal of Earth Sciences* 59(2), 180–186. DOI 10.3176/earth.2010.2.07
- KARATAJŪTĖ-TALIMAA, V., VALIUKEVIČIUS, J. & BRAZAUSKAS, A. 1987. Distribution of conodonts and vertebrates in the Silurian of Lithuania. *Geologija* 8, 59–71.
- KUMP, L.R. & ARTHUR, M.A. 1999. Interpreting carbon-isotope excursions: carbonates and organic matter. *Chemical Geology* 161, 181–198. DOI 10.1016/S0009-2541(99)00086-8
- LAPINSKAS, P. 2000. *Lietuvos silūro sandara ir naftingumas*. 203 pp. Geologijos institutas, Petro ofsetas, Vilnius.
- LOYDELL, D.K. 1998. Early Silurian sea-level changes. *Geological Magazine* 135(4), 447–471. DOI 10.1017/S0016756898008917
- LOYDELL, D.K., GUTIÉRREZ-MARCO, J.C. & ŠTORCH, P. 2023. The Sommerodde (Telychian, Silurian) positive carbon isotope excursion: why is its magnitude so variable? *Journal of the Geological Society* 180(5), 11 pp. DOI 10.1144/jgs2023-037
- MCLAUGHLIN, P.I., EMSBO, P., BRETT, C.E., BANCROFT, A.M., DESROCHERS, A. & VANDENBROUCKE, T.R. 2019. The rise of pinnacle reefs: A step change in marine evolution triggered by perturbation of the global carbon cycle. *Earth and Planetary Science Letters* 515, 13–25. DOI 10.1016/j.epsl.2019.02.039
- MÄNNIK, P., MEIDLA, T. & HINTS, O. 2024. Silurian stratigraphy in Estonia, 60–64. In HINTS, O., MÄNNIK, P. & TOOM, U. (eds) *11<sup>th</sup> Baltic Stratigraphic Conference, August 19–21, 2024, Tartu, Estonia. Abstracts and Field Guide*.
- MARWAN, N. & KURTHS, J. 2002. Nonlinear analysis of bivariate data with cross recurrence plots. *Physics Letters A* 302(5–6), 299–307. DOI 10.1016/S0375-9601(02)01170-2
- MARWAN, N. & KURTHS, J. 2004. Cross recurrence plots and their applications, 101–139. In BENTON, C.V. (ed.) *Mathematical physics research at the cutting edge*, Nova Science Publishers Inc. DOI 10.1007/s11071-013-1124-0
- MARWAN, N., THIEL, M. & NOWACZYK, N.R. 2002. Cross recurrence plot based synchronization of time series. *Nonlinear Processes in Geophysics* 9, 325–331. DOI 10.5194/npg-9-325-2002
- MARWAN, N., ROMANO, M.C., THIEL, M. & KURTHS, J. 2007. Recurrence plots for the analysis of complex systems. *Physics Report* 438, 237–329. DOI 10.1016/j.physrep.2006.11.001
- MELCHIN, M.J., SADLER, P.M. & CRAMER, B.D. 2020. The Silurian Period, 695–732. In GRADSTEIN, F.M., OGG, J.G., SCHMITZ, M.D. & OGG, G.M. (eds) *Geologic Time Scale 2020*. Elsevier. DOI 10.1016/B978-0-12-824360-2.00021-8
- MUNNECKE, A. & MÄNNIK, P. 2009. New biostratigraphic and chemostratigraphic data from the Chicotte Formation (Llandoverly, Anticosti Island, Laurentia) compared with the Viki core (Estonia, Baltica). *Estonian Journal of Earth Sciences* 58, 159–169. DOI 10.3176/earth.2009.3.01
- PAŠKEVIČIUS, J. & BRAZAUSKAS, A. 1987. Stratigraphic framework for marine and lagoonal shallow-water Silurian rocks of eastern Lithuania. *Geologija* 8, 10–28.
- PAŠKEVIČIUS, J., LAPINSKAS, P., BRAZAUSKAS, A., MUSTEIKIS, P. & JACYNA, J. 1994. Stratigraphic revision of the regional stages of the Upper Silurian part in the Baltic Basin. *Geologija* 17, 64–87.
- RADZEVIČIUS, S., SPIRIDONOV, A., BRAZAUSKAS, A., NORKUS, A., MEIDLA, T. & AINSAAR, L. 2014. Upper Wenlock  $\delta^{13}\text{C}_{\text{carb}}$  chemostratigraphy, conodont biostratigraphy and palaeoecological dynamics in the Ledai-179 drill core (Eastern Lithuania). *Estonian Journal of Earth Sciences* 63(4), 293–299. DOI 10.3176/earth.2014.33
- RADZEVIČIUS, S., TUMAKOVAITĖ, B. & SPIRIDONOV, A. 2017. Upper Homerian (Silurian) high-resolution correlation using cyclostratigraphy: an example from western Lithuania. *Acta Geologica Polonica* 67(2), 307–322. DOI 10.1515/agp-2017-0011

- RADZEVIČIUS, S., RACZYŃSKI, P., GARBARAS, A., CICHON-PUPIENIS, A. & ŽELVYS, T. 2024. Integrated stratigraphy of the Llandovery-Wenlock Boundary in the Łopianka-2 outcrop of the Sudeten Mountains, southwest Poland. *Lethaia* 57(2), 1–9. DOI 10.18261/let.57.2.8
- RINKEVIČIŪTĖ, S., STANKEVIČ, R., RADZEVIČIUS, S., MEIDLA, T., GARBARAS, A. & SPIRIDONOV, A. 2021. Dynamics of ostracod communities throughout the Mulde/lundgreni event: contrasting patterns of species richness and palaeocommunity compositional change. *Journal of the Geological Society* 179(1), jgs2021–039. DOI 10.1144/jgs2021-039
- SAMTLEBEN, C., MUNNECKE, A., BICKERT, T. & PÄTZOLD, J. 1996. The Silurian of Gotland (Sweden): facies interpretation based on stable isotopes in brachiopod shells. *Geologische Rundschau* 85(2), 278–292. DOI 10.1007/s005310050074
- SHACKLETON, N.J. & HALL, M.A. 1984. Carbon isotope data from Leg 74 sediments. *Initial Reports of the Deep Sea Drilling Project* 74, 613–619. DOI 10.2973/dsdp.proc.74.116.1984
- SIDARAVIČIENĖ, N., VALIUKEVIČIUS, J., PAŠKEVICIUS et al. 1999. *Lithuanian Stratigraphic Units*. 368 pp. Geological Survey of Lithuania, Vilnius.
- SPIRIDONOV, A., BRAZAUSKAS, A. & RADZEVIČIUS, S. 2015. The role of temporal abundance structure and habitat preferences in the survival of conodonts during the mid-early Silurian Ireviken mass extinction event. *PLoS ONE* 10(4), 1–24. DOI 10.1371/journal.pone.0124146
- SPIRIDONOV, A. 2017. Recurrence and cross recurrence plots reveal the onset of the Mulde event (Silurian) in the abundance data for Baltic conodonts. *The Journal of Geology* 125(3), 381–398. DOI 10.1086/691184
- SPIRIDONOV, A., KAMINSKAS, D., BRAZAUSKAS, A. & RADZEVIČIUS, S. 2017a. Time hierarchical analysis of the conodont paleocommunities and environmental change before and during the onset of the lower Silurian Mulde bioevent – A preliminary report. *Global and Planetary Change* 157, 153–164. DOI 10.1016/j.gloplacha.2017.09.002
- SPIRIDONOV, A., STANKEVIČ, R., GEČAS, T., ŠILINSKAS, T., BRAZAUSKAS, A., MEIDLA, T., AINSAAR, L., MUSTEIKIS, P. & RADZEVIČIUS, S. 2017b. Integrated record of Ludlow (Upper Silurian) oceanic geobioevents – Coordination of changes in conodont, and brachiopod faunas, and stable isotopes. *Gondwana Research* 51, 272–288. DOI 10.1016/j.gr.2017.08.006
- SPIRIDONOV, A., BALAKAUSKAS, L., STANKEVIČ, R., KLUCZYNSKA, G., GEDMINIENĖ, L. & STANČIKAITĖ, M. 2019. Holocene vegetation patterns in the southern Lithuania indicate astronomical forcing on the millennial and centennial time scales. *Scientific Reports* 9(1), 14711. DOI 10.1038/s41598-019-51321-7
- SPIRIDONOV, A., SAMSONĖ, J., BRAZAUSKAS, A., STANKEVIČ, R., MEIDLA, T., AINSAAR, L. & RADZEVIČIUS, S. 2020. Quantifying the community turnover of the uppermost Wenlock and Ludlow (Silurian) conodonts in the Baltic Basin. *Palaeogeography, Palaeoclimatology, Palaeoecology* 549, 1–18. DOI 10.1016/j.palaeo.2019.03.029
- STANKEVIČ, R., VENCKUTĖ-ALEKSIENĖ, A., RADZEVIČIUS, S. & SPIRIDONOV, A. 2024. Phytoplankton and zooplankton paleocommunity change before and during the onset of the Lau Extinction Event (Ludlow, Silurian). *Marine Micro-paleontology* 189, 102368. DOI 10.1016/j.marmicro.2024.102368
- SUNDBLAD, E.T. & VISSER, K. 2004. The Geologic History of the Carbon Cycle. *Treatise on Geochemistry* 8, 425–472. DOI 10.1016/B0-08-043751-6/08133-0
- WALASEK, N., LOYDELL, D.K., FRÝDA, J., MÄNNIK, P. & LOVERIDGE, R.F. 2018. Integrated graptolite-conodont biostratigraphy and organic carbon chemostratigraphy of the Llandovery of Kallholn quarry, Dalarna, Sweden. *Palaeogeography, Palaeoclimatology, Palaeoecology* 508, 1–16. DOI 10.1016/j.palaeo.2018.08.003
- WEBBER, C.L., JR. & MARWAN, N. 2015. *Recurrence quantification analysis. Theory and best practices*. 421 pp. Springer. DOI 10.1007/978-3-319-07155-8
- WENZEL, B. & JOACHIMSKI, M.M. 1996. Carbon and oxygen isotopic composition of Silurian brachiopods (Gotland/Sweden): palaeoceanographic implications. *Palaeogeography, Palaeoclimatology, Palaeoecology* 122(1–4), 143–166. DOI 10.1016/0031-0182(95)00094-1
- YAN, G., LEHNERT, O., MÄNNIK, P., CALNER, M., LI, L., WEI, X., GONG, F., LUAN, X. & WU, R. 2025. New bio-and chemostratigraphic data from southwestern China and its relation to Telychian (Llandovery, Silurian) climate change. *Palaeogeography, Palaeoclimatology, Palaeoecology* 662, 112740. DOI 10.1016/j.palaeo.2025.112740
- ŽELVYS, T., BRAZAUSKAS, A., SPIRIDONOV, A., BALČIŪNAS, M., GARBARAS, A. & RADZEVIČIUS, S. 2022. Stable carbon isotope stratigraphy of the Silurian in the Jočionys-299 borehole (eastern Lithuania). *Estonian journal of earth sciences* 71(3), 127–134. DOI 10.3176/earth.2022.09

## Supplementary electronic material

### Appendix 1. Carbon isotope data from the Ledai-179 borehole.